Deuteron spin-lattice relaxation for HD in solid argon

Joseph Ganem,* Peter A. Fedders, and R. E. Norberg
Department of Physics, Washington University, St. Louis, Missouri 63130
(Received 27 August 1992)

Measurements, using 55-MHz deuteron magnetic resonance (DMR), are reported of deuteron spin-lattice relaxation times for HD in solid argon at concentrations of 300–1100 ppm over the temperature range of 10–70 K. The relaxation times increase rapidly, from 10 to 4000 sec, as the temperature is reduced and are independent of the sample's para-D_2 concentration. Comparisons of deuteron spin-lattice relaxation times for HD in solid argon are made with previously reported relaxation times for solid HD–n-D_2 mixtures and for ortho-H_2 and para-D_2 in solid argon. The very different relaxation behavior for HD can be understood because it is an asymmetric molecule. The lack of exchange symmetry results in an increasing probability of the molecule being in a $J=0$ rotational state as the temperature is reduced. Nuclear spin-lattice relaxation in HD arises from phonon-induced Δm_J transitions for those molecules in the $J=1$ states. A theory is presented to calculate the nuclear spin-lattice relaxation rate $(1/T_1)$ in terms of a molecular decay rate (Γ) that arises from Δm_J or ΔJ transitions. The decay rate Γ as a function of temperature is determined from the relaxation data. It is found that the asymmetric rotor HD molecules have a coupling to the lattice phonons that is much stronger than for ortho-H_2 and para-D_2.

INTRODUCTION

As a complement to previous work[1,2] on the nuclear-spin relaxation of ortho-H_2 and para-D_2 matrix-isolated in solid argon, we have studied the deuteron magnetic resonance (DMR) of HD in argon. For ortho-H_2 and para-D_2 in solid argon, the nuclear spin-lattice relaxation rate is controlled through intramolecular interactions by the interaction of the molecule's angular momentum with the lattice phonons. The interaction of the molecular angular momentum with the lattice phonons can be characterized by a set of molecular decay rates Γ, and calculations have shown that knowledge of nuclear spin-lattice relaxation times can be used to determine the molecular decay rates.[3] For ortho-H_2 and para-D_2 in argon, the molecular decay rates arise from phonon-induced reorientations of the molecule's angular momentum, Δm_J transitions. Therefore, the nuclear spin-lattice relaxation rate $(1/T_1)$ is controlled by the rate at which the molecules undergo Δm_J transitions $\Gamma(\Delta m_J)$.[1,2] The temperature dependence of the rate $\Gamma(\Delta m_J)$ can be understood in terms of a model for anharmonic phonon quadrupolar interactions by Walker and van Kranendonk.[4,5] This paper examines the applicability of previous analyses of the nuclear spin-lattice relaxation of ortho-H_2 and para-D_2 in solid argon to the deuteron relaxation of HD in solid argon. There is a fundamental difference between HD and the ortho-H_2 and para-D_2 molecules previously studied. The population of HD molecules in a $J=1$ rotational state varies more dramatically with temperature. For ortho-H_2 and para-D_2 (both $J=1$ molecules at low temperatures) exchange symmetry forbids transition to the $J=0$ rotational ground state. The usual conversion of ortho-H_2 to para-H_2 (1.90% per hour[6]) and para-D_2 to ortho-D_2 (0.060% per hour[6]) is slow compared to the time scales of the experiments. In contrast, HD has no ortho-para distinction. At solid argon temperatures (well below 84 K) most HD molecules are in the rotational ground state. Since HD in the ground state lacks m_J degeneracy and cannot undergo Δm_J transitions, nuclei in isolated ground-state molecules relax primarily via molecular transitions to higher-J states. Therefore examination of the nuclear spin-lattice relaxation of matrix isolated HD, leads to an understanding of how higher molecular J states affect nuclear relaxation rates.

EXPERIMENTAL PROCEDURE

Measurements were made using 55-MHz pulsed deuteron NMR in an 8.5-T superconducting magnet. A detailed description of the spectrometer used in the experiments has been given by Mohr.[2] A liquid helium flow Dewar was used to control the temperature of the samples. The temperature was regulated by controlling the liquid-helium flow and the current through a heater wire in the vicinity of the sample. Temperatures above 10 K could be regulated to within ± 0.02 K. The temperatures of the samples were determined using a four-wire method to measure the resistance across two carbon-glass resistors. The resistors were placed at opposite corners of the sample chamber to check for temperature gradients. The triple point of D_2 was used to calibrate the resistors and temperature measurements were found to be accurate to within ± 0.1 K. Samples were made using procedures similar to those used by Conradi and co-workers[1,7,8] and Mohr.[2] A detailed account of the entire apparatus and procedure used in making the samples is given elsewhere.[9] Samples were made by dissolving HD in liquid argon and then freezing the argon over a period of a few minutes. The sample chamber was a 0.8-cm^3 cylinder made from Kel-F (3-M Co.) with a Teflon tube leading to the bottom of the sample chamber, which was used to introduce the HD gas. Prior to introduction of the HD

gas, the sample chamber was completely filled with liquid argon forcing the argon meniscus into an upper chamber 5 cm above the sample. The upper chamber was made of copper in order to shield any NMR signal it could produce. The purpose of the upper chamber was to improve sample homogeneity by providing a large volume in which escaping HD gas bubbles could break at the surface. HD gas was slowly (over a period of 10 min or so) introduced to the sample chamber. Then the HD gas was forced into solution by running a recirculation pump counter to the direction of the bubble flow, while slowly (over a period of 30–45 min) increasing the HD partial pressure. After most of the HD was dissolved [as seen by the very long T_1 (10 sec) compared to the HD gas ($T_1 \approx 10$ msec)] the sample was frozen. Freezing was accomplished by reducing the temperature of the sample at a rate of roughly 1 K/min until 20 K was reached. Approximately half of the dissolved HD was expelled during the freezing process. The expelled and excess gas was pumped out of the sample chamber. Sample concentrations were determined by comparing the fully relaxed DMR signal for HD in solid argon to that for a known pressure of HD gas. Using the ideal gas law and Curie's law, the number of HD molecules that produced a given signal intensity was calculated. Measurements of T_1 were made by determining the signal intensity from a steady-state sequence of 90° pulses. Variations were made in the repetition interval between the pulses and the resulting variation in signal intensity was fitted to a single exponential recovery function using a nonlinear least-squares-fitting routine. There was no observed nonexponential recovery of the DMR signal associated with the HD.

OVERVIEW OF THE DATA

Deuteron relaxation times for HD in solid argon were measured over a temperature range from 10 to 70 K in six samples with compositions varying from 300 to 1100 ppm. The compositions of the samples are listed in Table I. The deuteron T_1's for the HD signal in all of the samples are shown in Fig. 1(a). To within experimental error the T_1's show no sample dependence. The range of T_1's measured is from 10 to several thousand seconds. The deuteron T_1's increase as the temperature is reduced (increasing most rapidly below 20 K). Shown in Fig. 1(b) are the normalized M_0T products (product of the fully recovered signal intensity and the temperature normalized to 1), which are found to be constant from 10 to about 50 K. Above 50 K the argon begins to diffuse on the time scale of the experiments and the HD begins to escape.

TABLE I. Concentration in parts per million (ppm) of HD in each of the samples.

Sample	HD (ppm)
1	500
2	700
3	300
4	1000
5	800
6	1100

Three sources of HD gas were used in making the samples. Samples 1–4 were made with HD gas containing 3% n-D_2 (normal deuterium). Sample 5 was made with HD gas containing 2% n-D_2 and sample 6 was made from HD gas containing 10% n-D_2. As seen in Fig. 1(a), to within the scatter of the data there was no effect on the HD deuteron relaxation times from varying the amount of D_2 in the sample. In sample 6, which had enough D_2 signal to be observed by NMR, the para-D_2 and HD could be seen relaxing separately. Figure 2 shows two line shapes from sample 6 at 18.5 K. The top line shape [Fig. 2(a)] is after a 6.5-sec recovery time following saturation. The broad line is the fully recovered para-D_2 signal. The spike in the center is the beginning recovery of the HD signal. The bottom line shape [Fig. 2(b)] is after a 75-sec recovery following saturation. The line from the HD has recovered at its own rate to now dwarf the relatively unchanged para-D_2 line. Overall the deuteron line width for HD in argon is much narrower than the line width for para-D_2 in argon. The full width at half maximum for the para-D_2 line in Fig. 2(a) is about 500 Hz. With a correction for the 5-msec decay resulting from the magnet inhomogeneity, this corresponds to a T_2 for

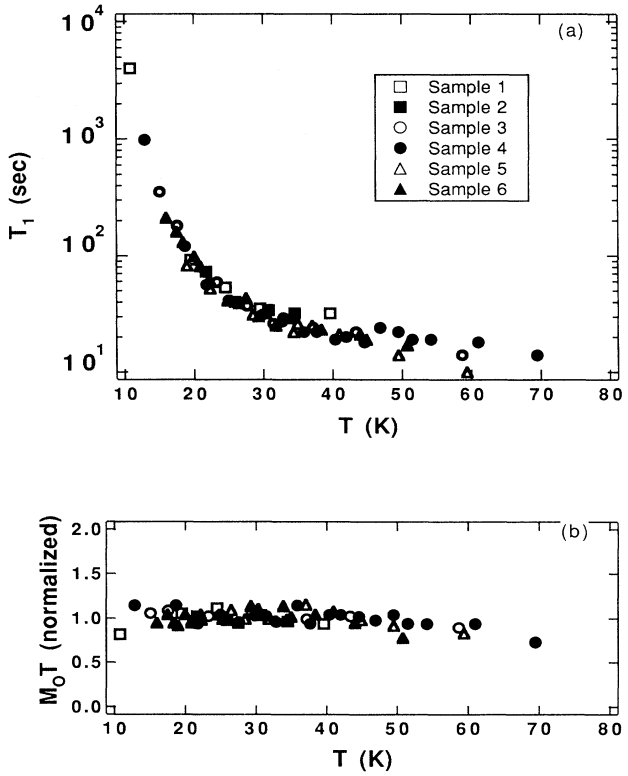

FIG. 1. (a) Deuteron T_1 data as a function of temperature for HD in argon. For the six samples studied, to within the scatter of the data, T_1 has no sample dependence. The sample compositions are listed in Table I. (b) The corresponding M_0T products remain constant until about 50 K. At temperatures above 50-K HD begins to escape.

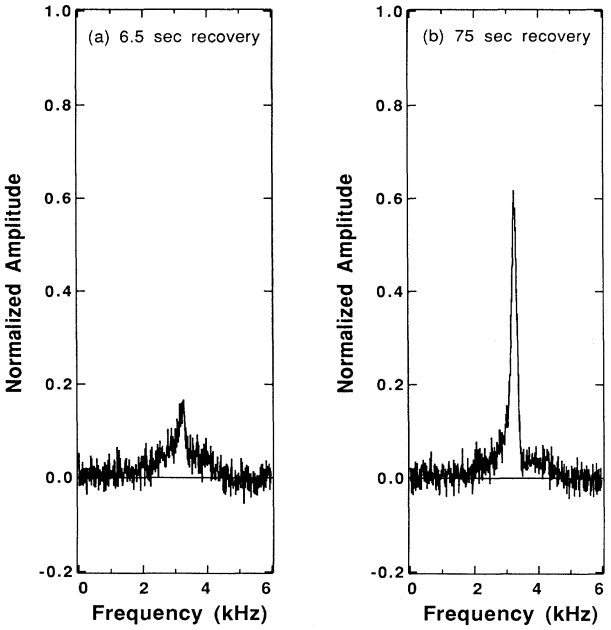

FIG. 2. The separate relaxations of HD and D_2 in solid argon. Shown are two line shapes from sample 6 at 18.5 K. (a) The recovery of the signal 6.5 sec following saturation with a 90° pulse. The broad line is the fully recovered para-D_2. (b) The recovery of the signal 75 sec following saturation with a 90 ° pulse. The slower relaxing HD has recovered and now dwarfs the relatively unchanged para-D_2 line.

para-D_2 in argon at 18.5 K of about 0.7 msec, in agreement with previous measurements by Mohr[2] who reported T_2 for para-D_2 in argon to be about 1 msec near this temperature. In contrast the linewidth of the HD in argon in Fig. 2(b) is limited by the magnet. Measurements of the deuteron T_2 for HD in argon using echoes are shown in Fig. 3. For HD in argon T_2 is between 20 and 40 msec and has little dependence on temperature. The intrinsic linewidths primarily reflect the quadrupolar interaction of the HD molecule with surrounding crystal fields. Consequent shifting of the molecular-angular momentum levels in turn shifts the deuteron nuclear Zeeman levels. HD molecules, their spherical symmetry arising from being predominantly in a ground state, interact more weakly with the crystal fields than do the oblong shaped para-D_2 molecules.

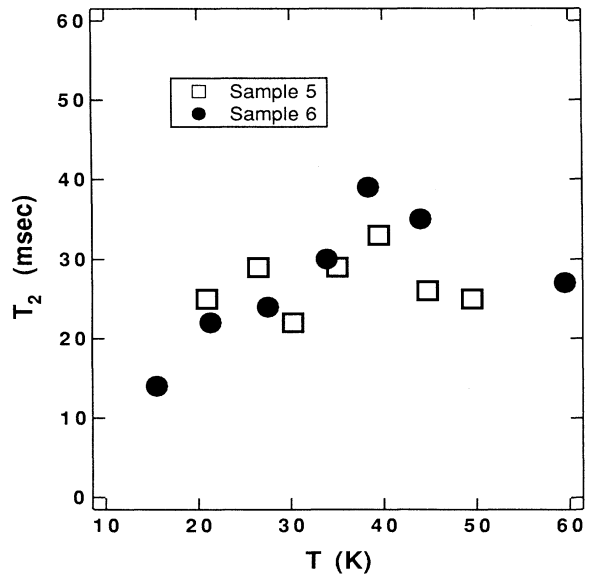

FIG. 3. Deuteron T_2 times for HD in argon. Open squares are measurements from sample 5. Dark circles are measurements from sample 6.

DISCUSSION: RELAXATION MECHANISMS FOR HD

Understanding the relaxation of HD in argon is more complicated than understanding the relaxation of ortho-H_2 and para-D_2 in argon because the $J=1$ to 0 transition is not forbidden for HD as it is for the symmetric molecules. A comparison of deuteron relaxation times for HD in argon to relaxation times for ortho-H_2 and para-D_2 in argon reveals radically different behavior for HD. Figure 4 compares deuteron T_1 times for HD in argon at 55 MHz to T_1 times previously reported for para-D_2 in argon at 55 MHz (Ref. 2) and ortho-H_2 in argon at 20 MHz

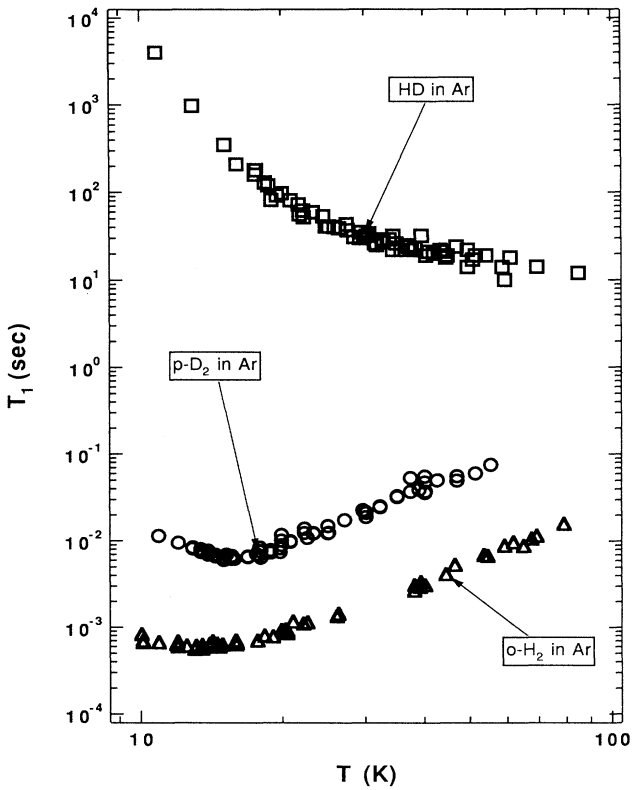

FIG. 4. Comparison of deuteron T_1's for HD in argon (open squares) with T_1's for ortho-H_2 in argon (open triangles) from Ref. 1 and para-D_2 in argon (open circles) from Ref. 2. In contrast to the symmetric molecules, T_1 for HD in argon increases monotonically as the temperature is reduced, exhibiting no T_1 minimum. Over the range of temperatures shown, the deuteron relaxation times for HD at 55 MHz are between 2 and 5 orders of magnitude longer than the corresponding relaxation times for para-D_2, which are also at 55 MHz.

(Ref. 1). In contrast to HD in argon, which has a monotonically increasing T_1 as the temperature is reduced, there is a T_1 minimum between 10 and 20 K for both para-D_2 and ortho-H_2 in argon. Also seen in Fig. 4, is that the deuteron T_1 for HD in argon is several orders of magnitude longer than T_1 for the other two molecules. To gain insight into the very different relaxation behavior of HD it is useful to compare the deuteron relaxation times for HD in argon to those for solid HD.

Deuteron relaxation times, also at 55 MHz, for solid HD have been reported previously.[10] In contrast to HD in argon, deuterons in solid HD can relax via spin diffusion to the para-D_2 molecules present. Consequently deuteron relaxation times for solid HD depend on the para-D_2 concentration. Figure 5 compares T_1 as a function of temperature for solid HD containing 10% n-D_2, 3% n-D_2, and 2% n-D_2 to T_1 for HD in argon, where the HD used in preparing the samples contained the same percentages of n-D_2. At temperatures below 11 K, the deuteron spin-lattice relaxation for solid HD varies little

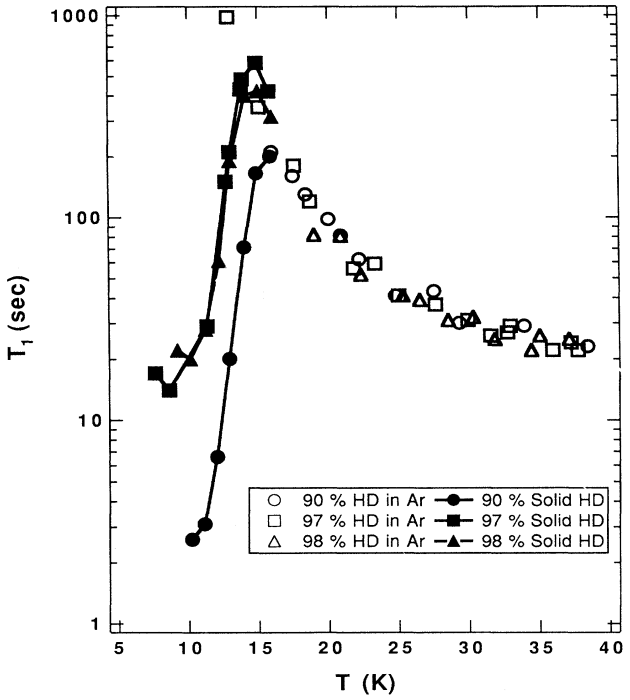

FIG. 5. Relaxation times from Ref. 10 for three different mixtures of HD–n-D_2, containing 90 at. % HD (circles), 97 at. % HD (squares), and 98 at. % HD (triangles), as solids (open markers) compared to HD gas with these same compositions matrix isolated in solid argon (solid markers). For solid mixtures of HD–n-D_2, the spin-lattice relaxation times decrease as the temperature is reduced and below 11 K are controlled by the para-D_2 concentration. For the same mixtures matrix isolated in solid argon, relaxation times increase monotonically as the temperature is reduced and are independent of para-D_2 concentration. Between about 14 K and the melting point of HD at 16.6 K, relaxation times for solid HD–n-D_2 mixtures are also independent of para-D_2 concentration and coincide with those for matrix isolated HD.

with temperature and is controlled by the concentration of para-D_2. Above 11 K there is a rapid increase in T_1 as the temperature is raised because thermally activated self-diffusion motionally narrows the resonant lines and makes spin diffusion to para-D_2 molecules a less effective relaxation mechanism. However, at temperatures just below the melt (between 14 and 16.6 K), T_1 for solid HD begins to decrease and, as seen in Fig. 5, is independent of the para-D_2 concentration and coincides with the T_1 for HD in argon for this temperature range.

A model developed by Bloom[11] to explain proton relaxation in solid HD with ortho-H_2 impurities and extended by Weinhaus *et al.*[12] to explain relaxation in solid ortho-para D_2 mixtures, also to a great extent explains deuteron relaxation in HD with para-D_2 impurities.[10] The model assumes that nuclei in isolated molecules in the $J=0$ state (HD and ortho-D_2), have intrinsic relaxation times that are effectively infinite, since these molecules cannot induce relaxation by undergoing Δm_J transitions. Only by transfer of energy to nuclei in $J=1$ molecules (spin diffusion) or, at sufficiently high temperatures, actual movement of the molecules themselves (self-diffusion) can nuclear spin-lattice relaxation occur. At the temperatures at which HD is solid it is assumed that essentially all the HD molecules are in the $J=0$ state. Therefore in solid HD, there should be a rapid rise in T_1 as the temperature is raised as well as when the concentration of $J=1$ molecules is lowered because in each case there is a decrease in the rate of spin diffusion. Since the model assumes that isolated HD molecules have nuclei with infinite relaxation times, the model predicts that T_1 can be made arbitrarily long by making the concentration of para-D_2 in the sample arbitrarily low. To account for the lack of dependence of T_1 on the para-D_2 concentration at temperatures just below the melt, previous work[10] has assumed that a HD molecule has an intrinsic relaxation. The additional relaxation can be accounted for by introducing an additional term into Bloom's model. The coincidence, shown in Fig. 5, of the HD in argon T_1 with the upper limit for the solid HD T_1, suggests that the intrinsic relaxation time for solid HD is the relaxation time for HD in argon. Motional narrowing in warm solid HD, reduces the spin diffusion rate and isolates the HD from the para-D_2 with relaxation results similar to those for HD isolated from each other by dilution in solid argon.

Examination of data for the relaxation of deuterons in HD in argon and solid HD suggests that there is an intrinsic relaxation time for nuclei in isolated HD molecules. We expect the intrinsic nuclear relaxation of HD to arise from the molecule making transitions to higher J states. Previous calculations[13,14] of the effects of higher J states on relaxation times for nuclear spins in hydrogen molecules have assumed that the observed spin-lattice relaxation rate can be calculated by averaging spin-lattice relaxation rates associated with each J state, over all the J states, using the appropriate weighting factor that reflects the population of each J state. That is,

$$\frac{1}{T_1} = \sum_j P(J) \frac{1}{T_1(J)} ,$$

where

$$P(J)=\frac{(2J+1)e^{-J(J+1)\Theta/T}}{\sum_j (2J+1)e^{-J(J+1)\Theta/T}} . \quad (1)$$

For ortho-H_2 and para-D_2 this sum would only be over odd J but for HD this sum would be over all J. For HD we will assume that $1/T_1$ ($J=0$ HD) = 0 and that at the temperatures of this experiment (<100 K) the population of HD molecules with $J>1$ is small. Under these assumptions Eq. (1) reduces to

$$\frac{1}{T_1}=\left[\frac{3e^{-2\Theta/T}}{1+3e^{-2\Theta/T}}\right]\frac{1}{T_1(J=1\text{HD})} , \quad (2)$$

where $1/T_1(J=1$ HD) is the relaxation rate for a $J=1$ HD molecule. Therefore, for HD in argon, the relaxation rate is proportional to the population of molecules in the $J=1$ state, which decreases exponentially as the temperature is reduced.

It is possible that there could be two relaxation rates, one for the molecules in the higher J state that is relatively fast and one for the ground-state molecules that is much slower. However, as seen in Fig. 1(b), M_0T is constant over most of the temperatures studied. If there was a population of molecules with nuclei relaxing either too fast or too slow compared to the time scale of the T_1 measurements, M_0T would have an exponential temperature dependence. We monitor the recovery of the same number of HD molecules, and they are observed to have a common relaxation time (single T_1). Therefore the rate of the ΔJ transitions $\Gamma(\Delta J)$ is fast compared to the relaxation rate ($1/T_1$).

We assume then that there is a single relaxation rate that, according to Eq. (2), is proportional to the probability of finding a HD molecule in a $J=1$ state. Equation (2) can be used to calculate relaxation times for $J=1$ HD molecules from the observed relaxation times if Θ is known. For a free HD molecule Θ is 64.2 K. However, by matrix isolating HD, the static crystal fields from the argon environment could admix a $J=1$ component into the rotational ground state and possibly change the energy difference between the ground and first excited state. The admixture of higher J states into the rotational ground state is known to occur for HD in amorphous silicon. Volz *et al.*[15] discovered unusual multiple deuteron spin echoes arising from HD trapped in amorphous silicon over a temperature range from 10 to 100 K. For these echoes to form there must be an admixture of $J=1$ into the rotational ground state in order for the molecule to have nonzero intramolecular quadrupolar and dipolar coupling constants. For HD in argon there are no detectable deuteron multiple echoes. The crystal-field interaction at the HD sites in argon is not an appreciable fraction of the 128 K ΔJ splitting and the admixture of $J=1$ into the rotational ground state needed to produce a detectable multiple echo component is insufficient. Therefore, we expect that the ground state is primarily a pure $J=0$ state and that Θ for HD in argon is very close to that of a free HD molecule.

Assuming that Θ for HD in argon is 64.2 K, Fig. 6 illustrates the deuteron $T_1(J=1$ HD) times deduced for HD in argon (open squares) and plots for comparison the T_1 times for para-D_2 in argon[2] (open circles) and the T_1 times for ortho-H_2 in argon[1] (open triangles). The HD in argon deuteron $T_1(J=1$ HD) times are nearly two orders of magnitude larger than the para-D_2 times at the same Larmor frequency. Inspection of Fig. 6 also reveals, that in contrast to the ortho-H_2 and para-D_2 molecules, there is no $T_1(J=1$ HD) minimum over the 10–70 K temperature range. It appears that for this temperature range the correlation frequency of the fluctuation that induces deuteron nuclear relaxation in HD is much larger than the 3.4×10^8 sec^{-1} Larmor frequency.

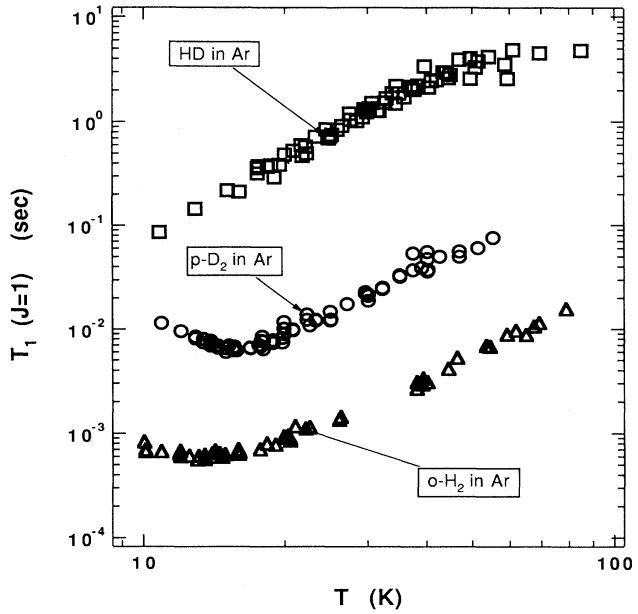

FIG. 6. Comparison of deuteron $T_1(J=1)$ times for HD in argon calculated from Eq. (2) (open squares), with T_1's for ortho-H_2 in argon (open triangles) from Ref. 1 and para-D_2 in argon (open circles) from Ref. 2.

RELAXATION OF ISOLATED $J=1$ HYDROGEN MOLECULES

The nuclear spin-lattice relaxation for $J=1$ H_2 molecules (ortho-H_2) in a solid nonmagnetic host has been calculated previously.[3] The calculation considered the effect that the static electric-field gradients from the host have on the reorientation rate of the molecular angular momentum (Δm_J transitions). It was shown that nuclear spin-lattice relaxation rates depend on the symmetry of the crystal-field gradients. Three symmetry cases were considered: cubic, axial, and no symmetry. The Hamiltonian connecting the nuclear spins to the molecular angular momentum can be written in terms of an expansion of multipole operators.[3] For the molecular angular momenta, each multipole operator has an associated correlation function characterized by a decay rate Γ. The nuclear spin-lattice relaxation rate can be expressed in terms of these decay rates. In practice only the $l=1$ (di-

polar) and $l=2$ (quadrupolar) operators need be considered. The results then are expressible in terms of the two decay rates Γ_1 and Γ_2, which characterize the interaction of the molecular angular momentum with the lattice phonons. Under most conditions any angular variation in the interaction of the molecules with the phonons can be neglected. Lack of an angular variation means that $\Gamma_2=0.6\Gamma_1$ for Δm_J transition. Knowledge of the relaxation times and the appropriate symmetry of the crystal-field gradients can be used to calculate the molecular decay rates.

The calculations for T_1 of H and D nuclear spins in HD are very similar to the calculations[3] for the relaxation of H and D nuclear spins in H_2 and D_2, respectively. Thus the details of the calculations will be omitted. We shall first present our results for the T_1 relaxation of H or D nuclei in a HD molecule in a $J=1$ state. There are three distinct contributions to these relaxation rates, namely the spin-rotation, quadrupolar, and dipolar contributions.

The spin-rotation Hamiltonian between the H (or D) nuclei and the molecular angular momentum can be written as

$$H_{\rm sr}=\hbar\omega_1\Sigma_m A^{\dagger}_{lm}B_{lm} ,$$
$$\omega_1=-\omega_c[2I(I+1)/9]^{1/2} , \tag{3}$$

where the A_{lm} and B_{lm} are the irreducible multipole operators for the molecular and nuclear spins, respectively, and I refers to the nuclear spin, where $\omega_c(H)=5.479\times10^5$ sec^{-1} and $\omega_c(D)=0.842\times10^5$ sec^{-1}. By methods used earlier[3] we obtain the HD spin-rotation relaxation rate $1/T^{\rm sr}_{1,J=1}$:

$$\frac{1}{T^{\rm sr}_{1,J=1}}=\frac{4}{3}\omega_c^2F_1(\omega_0) \tag{4}$$

in the case of cubic symmetry, where ω_0 is the frequency of the experiment and

$$F_l(\omega)=\Gamma_l/(\omega^2+\Gamma_l^2) \tag{5}$$

are the molecular correlation functions and Γ_l are the molecular relaxation rates. For molecules in environments of axial symmetry we obtain

$$\Gamma_1=\frac{2}{3}\omega_c^2(1-z^2)F_1(\omega_0) , \tag{6}$$

where z is the cosine of the angle between the magnetic field and the axis of the electric-field gradient (efg). For the case of no symmetry, we obtain

$$\Gamma_1=0 . \tag{7}$$

The above results were derived in our earlier work. Further, as in earlier work, cubic symmetry refers to a situation where all of the splittings arising from electric-field gradients are small compared to the Γ_l. The case of axial symmetry refers to the situation where one electric-field gradient is large compared to the Γ_l. If there are more than one large electric-field gradient, then no symmetry obtains.

The quadrupolar interaction of the nuclear spin with the molecular angular momentum is described by the Hamiltonian

$$H_q=\hbar\omega_2\Sigma_m A^{\dagger}_{2m}B_{2m} ,$$
$$\omega_2=\omega_Q/\sqrt{10}[I(I+1)(2I-1)(2I+3)]^{1/2} , \tag{8}$$

where ω_Q is zero for H and ω_Q(D) $=1.426\times10^5$ sec^{-1}. The relaxation rates (for D) in the case of cubic symmetry are

$$\frac{1}{T^q_{1,J=1}}=3\omega_Q^2[4F_2(2\omega_0-2\omega_x)+F_2(\omega_0-\omega_x)] , \tag{9a}$$

where $\omega_x=\gamma_mH_0$, γ_m is the gyromagnetic ratio for the HD molecule, and H_0 is the external magnetic field. For axial symmetry,

$$\frac{1}{T^q_{1,J=1}}=\tfrac{3}{2}\omega_Q^2\{3(1-z^2)^2F_2(2\omega_0)+\tfrac{1}{2}(z+1)^4F(2\omega_0-2\omega_xz)+\tfrac{1}{2}(1-z)^4F_2(2\omega_0+2\omega_xz)+3z^2(1-z^2)F_2(\omega_0)$$
$$+\tfrac{1}{2}(1-z^2)(1+z)^2F_2(\omega_0-2\omega_xz)+\tfrac{1}{2}(1-z^2)(1-z)^2F_2(\omega_0+2\omega_xz)\} . \tag{9b}$$

Finally, for no symmetry,

$$\frac{1}{T^q_{1,J=1}}=3\omega_4^2\{\tfrac{3}{2}(1-z^2)^2F_2(2\omega_0)+\tfrac{1}{4}(1+6z^2+z^4)F_2(2\omega_0)+\tfrac{1}{4}(1-z^2)rF_2(2\omega_0)$$
$$+F_2(\omega_0)[\tfrac{3}{2}z^2(1-z^2)+\tfrac{1}{4}(1-z^2)(1+z^2)-\tfrac{1}{4}(1-z^2)^2r]\} \tag{9c}$$

In Eq. (9c), as in earlier work, r varies between -1 and $+1$ and reflects the size of the off-diagonal elements of the electric-field-gradient tensor.

The dipolar coupling between the nuclear spins depends on the orientation of the molecular axis and thus on the molecular angular-momentum operators. The Hamiltonian can be written as

$$H_d=\hbar\omega''\{\sqrt{2}A_{2,0}[I_{1z}I_{2z}-\tfrac{1}{4}(I_{1+}I_{2-}+I_{1-}I_{2+})]+\tfrac{1}{2}\sqrt{3}[A_{2,2}I_{1-}I_{2-}+A_{2,-2}I_{1+}I_{2+}]$$
$$+\tfrac{1}{2}\sqrt{3}[A_{2,-1}(I_{1z}I_{2+}+I_{2z}I_{1+})]-[A_{2,1}(I_{1z}I_{2-}+I_{2z}I_{1-})]\} , \tag{10}$$

where $\omega''=2\gamma_1\gamma_2/5R^3$ and $I_{i\alpha}$ refers to the α component of spin species H or D. The results for the relaxation rates are, for cubic symmetry for spin I_1

$$\frac{1}{T^d_{1,J=1}} = \omega_2\{F_2(\omega_1-\omega_2)+6F_2(\omega_1+\omega_2-\omega_x)+3F_2(\omega_1-\omega_x)\}\ ,$$
$$\omega_d = \omega''[I_2(I_2+1)/3]^{1/2}\ . \tag{11a}$$

Here ω_1 is the resonant frequency under consideration (H or D), while ω_2 is the frequency of the other species (D or H).

For axial symmetry we obtain

$$\begin{aligned}\frac{1}{T^d_{1,J=1}} = \omega_d^2\{&\tfrac{1}{4}(3z^2-1)F_2(\omega_1-\omega_2)+\tfrac{3}{8}(1-z^2)^2[F_2(\omega_1-\omega_2-2\omega_x z)+F_2(\omega_1-\omega_2+2\omega_x z)]\\ &+\tfrac{9}{4}(1-z^2)^2F_2(\omega_1+\omega_2)+\tfrac{3}{8}(1+z)^4F_2(\omega_1+\omega_2-2\omega_x z)+\tfrac{3}{8}(1-z)^4F_2(\omega_1+\omega_2+2\omega_x z)\\ &+\tfrac{9}{2}z^2(1-z^2)F_2(\omega_1)+\tfrac{3}{4}(1-z^2)(1+z)^2F_2(\omega_1-2\omega_x z)+\tfrac{3}{4}(1-z^2)(1-z)^2F_2(\omega_1+2\omega_x z)\}\end{aligned} \tag{11b}$$

and, for no symmetry,

$$\begin{aligned}\frac{1}{T^d_{1,J=1}} = \omega_d^2\{&\tfrac{1}{4}(3z^2-1)^2F_2(\omega_1-\omega_2)+\tfrac{3}{8}(1-z^2)^2(1+r)F_2(\omega_1-\omega_2)+\tfrac{9}{4}(1-z^2)^2F_2(\omega_1+\omega_2)\\ &+\tfrac{3}{8}(1+6z^2+z^4)F_2(\omega_1+\omega_2)+\tfrac{3}{8}(1-z^2)^2rF_2(\omega_1+\omega_2)+\tfrac{9}{2}z^2(1-z^2)F_2(\omega_1)\\ &+\tfrac{3}{4}(1-z^2)(1+z^2)F_2(\omega_1)+\tfrac{3}{4}(1-z^2)(z^2-1)rF_2(\omega_1)\}\ .\end{aligned} \tag{11c}$$

If we sum over the H_{sr}, H_q, H_d rates, average over all angle, and look only at frequencies much greater or much less than the Γ_l, the expressions become much simpler. For example, we can write

$$\frac{1}{T_{1,J=1}} = A_1\Gamma_1/\omega^2\ ,\quad \omega \gg \Gamma_l\ ,$$
$$\frac{1}{T_{1,J=1}} = A_2/\Gamma_1\ ,\quad \omega \ll \Gamma_l\ . \tag{12}$$

The value of A_1 and A_2 in units of 10^{10} sec^{-2} are given in Table II for values of the f ratio Γ_2/Γ_1 equal to 0.6 and 1.0. Also given in Table II are the consequent predicted ratios $[T_1(H)/T_1(D)]_{J=1}$ for the symmetries and frequency ranges considered.

With the usual anharmonic-Raman Δm_J mechanism $f=0.6$. However, if the molecular relaxation is dominated by the changing of J states, $f=1$ and $\Gamma_1=\Gamma_2$ is the rate of the molecule going from $J=1$ to 0. To get the observed rate $1/T_1$ appropriate for either case, the $1/T_{1,J=1}$ expressions must be multiplied by the probability of being in the $J=1$ state, Eq. (2).

TABLE II. HD rate coefficients and $T_{1,J=1}$ ratios for cubic symmetry and for no symmetry.

A (units of 10^{10} sec^{-2})	Cubic symmetry $f=0.6$	Cubic symmetry $f=1.0$	No symmetry $f=0.6$	No symmetry $f=1.0$
A_1 (D)	169.2	270.0	3.18	5.30
A_1 (H)	56.9	60.5	1.79	2.98
A_2 (D)	57.4	34.8	22.6	13.5
A_2 (H)	54.0	48.4	5.78	3.45
	$[T_1(H)/T_1(D)]_{J=1}$ ratios			
$\omega \gg \Gamma_1$ and same H_0 for H and D	126	189	75.4	75.4
$\omega \ll \Gamma_1$	1.06	0.719	3.91	3.91

The nuclear relaxation data (Fig. 6) of Conradi, Luszczynski, and Norberg[1] and of Mohr[2] exhibit T_1 minima for o-H_2 and p-D_2 matrix isolated in solid Ar. Thus for H_2 and D_2 the molecular $\Gamma_{\Delta m_J}$ rates pass through the nuclear Larmor frequencies (20 and 55 MHz) as the temperature is decreased between 20 and 10 K. The magnitudes of the proton and deuteron T_1 times at the minima demonstrate that the observed o-H_2 and p-D_2 experience static electric-field gradients of low symmetry (the no symmetry case) and large compared to the nuclear Larmor frequencies (1.3 and 3.5×10^8 sec^{-1}, respectively). It is reasonable to anticipate that HD will be situated at similar sites in cold solid argon, with large static-electric field gradients of no symmetry. In this case the calculated results given in Table II predict HD ratios $[T_1(H)/T_1(D)]_{J=1}$ of either 3.9 or 75, depending on the magnitude of Γ_1. However, recent measurements by Lyou[16] have shown that, between 20 and 45 K, HD in solid Ar shows relaxation times $T_1(H)=T_1(D)$ in an 8.5-T field. The T_1 data are believed to be accurate to within 10%. From Table II, the indicated conclusion is that the HD nuclear relaxation in solid Ar takes place under conditions of cubic symmetry (small electric-field gradients), $f=\Gamma_2/\Gamma_1=0.6$, and $\Gamma_l \gg \omega$. We conclude that the HD molecular relaxation proceeds via a $\Gamma_{\Delta m_J}$ process and not a $\Gamma_{\Delta J}$ process, since for the latter case Γ_1 necessarily is equal to Γ_2 and $f=1$, contrary to Lyou's result.

The temperature variations of the HD-Ar deuteron T_1 (D) data in Figs. 4 and 6 are consistent with $\Gamma_l \gg \omega$, since no T_1(D) minimum is observed, and $T_{1,J=1}$(D) increases with increasing temperature in a manner similar to that for $T_1(o\text{-}H_2)$ and $T_1(p\text{-}D_2)$ on the warm sides of their T_1 minima. Accepting no symmetry, $f=0.6$, and $\Gamma_l \gg \omega$ for HD in solid Ar, Eq. (12) and the $T_{1,J=1}$ data of Fig. 6 yield the molecular $\Gamma_2(T)$ results plotted at the top of Fig. 7. The deduced HD molecular Δm_J rates are

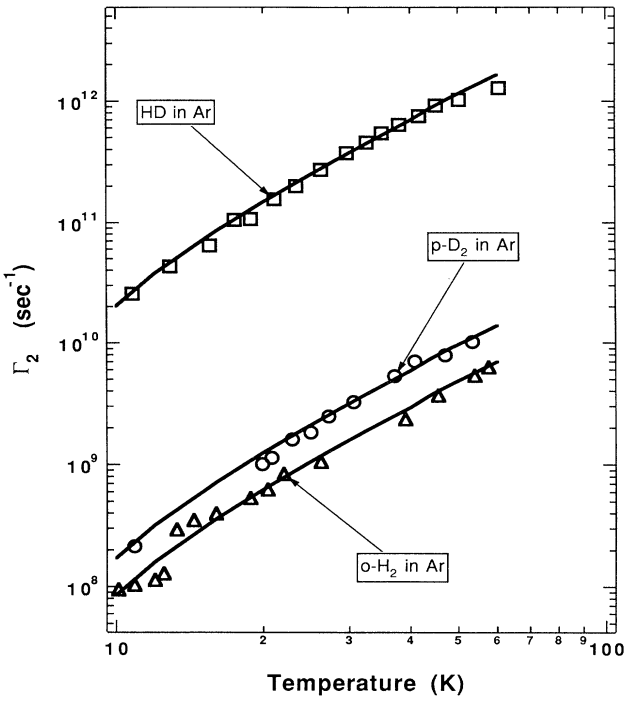

FIG. 7. Comparison of the temperature dependences of the molecular decay rates $\Gamma_2(J=1$ HD), Γ_2(ortho-H_2), and Γ_2(para-D_2) for these molecules in solid argon. The temperature dependence of Γ is very similar for all three molecules and arises from anharmonic Raman phonon coupling. The variation in the magnitude of Γ arises from each molecule having a different phonon-coupling coefficient C, defined by Eq. (13).

seen to be two orders of magnitude larger than those for o-H_2 and p-D_2 and range from 2×10^{10} to 1×10^{12} $\sec^{-1}$ between 12 and 60 K.

The temperature variations of the Γ_2 results in Fig. 7 can be fitted very well by assuming that the molecular Δm_J transitions result from anharmonic phonon quadrupolar interactions. The model of Van Kranendonk and Walker[5] then can be used to describe the temperature dependence of the molecular decay rate as

$$\Gamma_2(\Delta m_J)=CE^*(T^*)T^{*2}\ , \tag{13}$$

where C is the phonon coupling coefficient, $E^*(T^*)$ is a tabulated function, and T^* is a reduced temperature T/Θ_c. The temperature Θ_c is a characteristic of the host matrix for the hydrogen. Fits of the Fig. 7 $\Gamma_2(T)$ results to Eq. (13) yield phonon-coupling coefficients of $C_{H_2}=3.1\times10^9$ $\sec^{-1}$ for o-H_2 in argon,[1] $C_{D_2}=6.2\times10^9$ $\sec^{-1}$ for p-D_2 in argon,[2] and $C_{HD}=6\times10^{11}$ $\sec^{-1}$.

CONCLUSIONS

From the NMR T_1 data we conclude that the dominant HD molecular relaxation mechanism arises from reorientations of the molecular angular momentum (Δm_J transitions) and not from changes in the magnitude of the angular momentum (ΔJ transitions). This is generally to be expected for all of the hydrogens in Ar. Since the characteristic vibration frequency[1] of all of the hydrogens in Ar is about 40 K, the Debye temperature for Ar is 82 K, and the splitting between the $J=0$ and 1 states for HD is 128 K, it would require the emission or absorption of at least two phonons to aid the ΔJ transition. This makes such a process slow.

We also note that the molecular relaxation rate inferred for D_2 in Ar is twice the rate for H_2 in Ar. A factor of order 1 or 2 is about what one would expect given the mass difference and ensuing effects on vibrations. However, the molecular relaxation rate deduced for HD in Ar is two orders of magnitude greater than the relaxation rate for H_2 or D_2. The reason for this is that the center of mass (CM) and electrical or force center (FC) of the HD molecule are not the same but differ by about 0.12 Å. The molecule tends to rotate about its CM, but its equilibrium place in the lattice and force between it and its neighbors is determined by the position of the FC.

First let us consider the interaction of the angular momentum of an H_2 or D_2 molecule in a $J=1$ state with the surrounding lattice. Since the molecule is (slightly) asymmetric, the molecule pushes the surrounding Ar atoms as it rotates. (For Ar and for the hydrogens a reasonable view is that the molecules or atoms are essentially touching.) Now when the HD molecule rotates about its CM, the FC will move by about 0.25 Å. Thus the rotation must also be accompanied by a translation that tends to keep the FC near the equilibrium position. This combined rotational-translational motion gives the HD an effective radius that is considerably greater than the radius of a H_2 molecule. Since the molecule is tightly packed into the Ar lattice, this larger effective radius means that the rotational motion of the molecule will have a considerably larger effect on the surrounding Ar atoms. Thus the coupling constant for the HD angular momentum—phonon coupling will be increased and C, the phonon-coupling coefficient in Eq. (13), is proportional to the square of this coupling constant.

ACKNOWLEDGMENTS

The authors acknowledge helpful conversations with Mark Conradi. This work was supported in part by National Science Foundation (NSF) Low Temperature Physics Program Grant Nos. DMR-87-01515 and DMR-90-02857.

*Present address: Code 6540, Naval Research Laboratory, Washington, DC 20375.

[1]M. S. Conradi, K. Luszczynski, and R. E. Norberg, Phys. Rev. B **20**, 2954 (1979).

[2]G. A. Mohr, Ph.D. thesis, Washington University, St. Louis, 1986 (unpublished).

[3]P. A. Fedders, Phys. Rev. B **20**, 2588 (1979).

[4]J. Van Kranendonk, Physica **20**, 781 (1954).

[5]J. Van Kranendonk and M. B. Walker, Can. J. Phys. **46**, 2441 (1968).

[6]I. F. Silvera, Rev. Mod. Phys. **52**, 393 (1980).
[7]M. S. Conradi, Ph.D. thesis, Washington University, St. Louis, 1977 (unpublished).
[8]M. S. Conradi, K. Luszczynski, and R. E. Norberg, Phys. Rev. B **19**, 20 (1979).
[9]J. Ganem, Ph.D. thesis, Washington University, St. Louis, 1989 (unpublished).
[10]J. Ganem and R. E. Norberg, Phys. Rev. B **43**, 1 (1991).
[11]M. Bloom, Physica **23**, 767 (1957).
[12]F. Weinhaus, S. M. Myers, B. Maraviglia, and H. Meyer, Phys. Rev. B **3**, 626 (1971).
[13]P. A. Fedders, Phys. Rev. B **30**, 3603 (1984).
[14]R. E. Norberg, Phys. Rev. B **31**, 7925 (1985).
[15]M. P. Volz, P. Santos-Filho, M. S. Conradi, P. A. Fedders, R. E. Norberg, W. Turner, and W. Paul, Phys. Rev. Lett. **63**, 2582 (1989).
[16]J. H. Lyou, Ph.D. thesis, Washington University, St. Louis, 1991 (unpublished).